BIOCHEMICAL CYTOLOGY OF TRICHOMONAD FLAGELLATES

I. Subcellular Localization of Hydrolases, Dehydrogenases, and Catalase in *Tritrichomonas foetus*

MIKLÓS MÜLLER

From The Rockefeller University, New York 10021

ABSTRACT

To determine the localization of several enzymes in *Tritrichomonas foetus*, the axenic KV-1 strain was grown in Diamond's medium with bovine serum, homogenized in 0.25 M sucrose, and subjected to analytical differential and isopycnic centrifugation. The fractions were assayed for their enzymatic composition and examined electron microscopically. NADH and NADPH dehydrogenases, about 90% of the catalase, and two hydrolases, α-galactosidase and manganese-activated β-galactosidase I are in the nonsedimentable part of the cytoplasm. α-Glycerophosphate and malate dehydrogenases are associated with a large particle, whose equilibrium density in sucrose gradients is 1.24. This particle corresponds to that population of the paracostal and paraxostylar granules which, having a uniform granular matrix surrounded by a single membrane, resemble microbodies from other organisms. The small sedimentable portion of catalase (about 10% of the total activity) is not associated with these granules and equilibrates at density 1.22. The nature of the subcellular entity carrying catalase could not be ascertained. Hydrolases with a pH optimum around 6–6.5 (protease, β-*N*-acetylglucosaminidase, β-*N*-acetylgalactosaminidase, and cation-independent β-galactosidase II), as well as a large part of acid phosphatase, are associated with a population of large particles which equilibrate at densities from 1.15 to 1.20. The hydrolases in these granules lose their structure-bound latency easily after freezing and thawing. These particles correspond to another population of the paracostal and paraxostylar granules which have varied shape and inhomogeneous content with frequent myelin figures, indicating a digestive function. The rest of the phosphatase and most of the acid β-glucuronidase activity are in a smaller granule fraction with an equilibrium density around 1.18. The latency of these enzymes is quite resistant to freezing and thawing. This particle population consists of smaller, very often flattened vesicles and granules, many of which are clearly fragments of the prominent Golgi apparatus of the cell.

INTRODUCTION

Trichomonad flagellates parasitize the alimentary canal or urogenital apparatus of vertebrates and invertebrates. Their metabolism is anaerobic although many species exhibit intensive respiration under aerobiosis (10, 15, 34, 38). An important cytological correlate of their anaerobic nature is that typical mitochondria have not been demonstrated. Their cytoplasm contains a wide variety

of membrane-bounded organelles besides a highly complex flagellar apparatus (2, 8, 16, 19, 20, 25, 32, 39, 40). Some of these organelles, e.g. the paraxostylar and paracostal granules (chromatic granules) or the parabasal apparatus (Golgi complex), were already observed by light microscopy (26). Although a fair amount is known about the biochemistry of certain trichomonads (38), there is very little information on the enzymatic makeup and function of the subcellular organelles in these forms.

We report here our studies on a typical trichomonad, *Tritrichomonas foetus* (Riedmüller) 1928, employing biochemical, cell fractionation, and morphological methods. We thereby identified biochemically several types of subcellular organelles. Our main results deal with the enzyme content and morphological characterization of particles carrying dehydrogenases and of particles containing hydrolases. We also comment on the subcellular localization of catalase and of NADH and NADPH dehydrogenases.

METHODS

Organism and Culture

T. foetus KV-1 strain was cultured in Diamond's medium without agar, supplemented with 10% bovine serum (18). The cultures were harvested after growing 1 day at a cell density of about 10^6/ml.

Cell Fractionation

Mass cultures (up to 4 liter at one time) were harvested and washed with ice-cold 0.25 M sucrose in a Sorvall RC-3 centrifuge equipped with SS-34 or GS-3 rotors (Ivan Sorvall, Inc., Newtown, Conn.). Centrifugation was at 2,000 rpm for 5 min. The washed cells were taken up in cold sucrose and disrupted with 20–30 strokes in a Potter-Elvehjem tissue homogenizer fitted with a smooth Teflon pestle rotating at 1,000 rpm. This did not result in complete cell breakage but did give good preservation of subcellular particles in the homogenate. The homogenate was then fractionated by differential centrifugation with equipment and conditions as described for individual experiments.

Isopycnic centrifugation was used to subfractionate particle fractions from the homogenate. The preparation was layered over a continuous sucrose gradient extending linearly with respect to volume from 1.12 to 1.28 density and itself resting on a cushion of density of 1.32, in the automatic zonal rotor of Beaufay. Details of the method and calculation and presentation of results have been described (7, 28. 30).

Biochemical Assays

α-Glycerophosphate dehydrogenase was assayed spectrophotometrically with dichlorophenol-indophenol as electron acceptor at 30°C. The assay system contained 40 mM phosphate buffer, pH 7.5, 1.25 mM DL-α-glycerophosphate, 0.3 mM dye, and the enzyme sample. Change in absorbance (ϵ) at 600 nm was recorded first before, then after addition of substrate, and the difference between the two slopes was taken as a measure of enzyme activity; ϵ_{600} for the dye was taken as 16×10^3 M^{-1} cm^{-1}. Total NAD-linked malate dehydrogenase activity was determined by polarographic measurement of O_2 consumption at 37°C. The reaction mixture in the electrode vessel contained 55 mM imidazole buffer, pH 7.0, 10 mM L-malate, excess of NADH oxidase in the form of a high speed supernatant of *T. foetus* homogenate, and the enzyme sample. After recording the endogenous activity, NAD solution was injected into the chamber to a concentration of 20 μM. NADH and NADPH oxidases were determined spectrophotometrically at 30°C in a system containing 66 mM imidazole buffer, pH 7.0, 200 μM NADH or NADPH, and the enzyme sample. The change in absorbance at 340 nm was recorded; ϵ_{340} for NADH or NADPH is 12.2×10^3 M^{-1} cm^{-1}. Catalase was assayed at 0°C by the method of Baudhuin et al. (5).

Details of the assays for the hydrolases are given in Tables I and II. The two β-galactosidases described by Harrap and Watkins (23) were distinguished on the basis of the effect of Mn^{2+} and EDTA on their activity. According to these authors, the activity of the manganese-dependent β-galactosidase I, taken as 100 without addition, is increased to 200 by 2 mM Mn^{2+} and decreased to 20 by 2 mM EDTA; corresponding values for the cation-independent β-galactosidase II are 105 and 112. Since the purified enzymes were not available to us, we calculated the distributions of the two β-galactosidases from data obtained in the presence of either Mn^{2+} or EDTA, assuming the validity of the above values for our strain. Protein was determined by an automated Lowry procedure with bovine serum albumin as standard (28).

Enzyme units are defined as the amount of enzyme necessary to release 1 μmol product per min under the assay conditions. Protease activity is expressed as chromogenic equivalents of 1 μg of albumin released per min. Unit of catalase is the enzyme amount necessary to decompose 90% of H_2O_2 present in a total volume of 50 ml per min (5).

Electron Microscopy

Intact cells, still in the culture medium, were fixed for 20 min or longer at 0°C by adding an equal

volume of 4% glutaraldehyde buffered with 100 mM phosphate, pH 7.4. The fixed cells were gently concentrated in an International clinical model centrifuge (International Scientific Instruments Inc., Palo Alto, Calif.) and transferred into a Microfuge tube which was spun for 5 min at top speed in the Microfuge (Beckman Instruments, Inc., Fullerton, Calif.) to obtain a firm pellet. The tube was cut into small pieces, and these were handled with the adhering pellet as are tissue pieces.

TABLE I

*Incubation Conditions for Hydrolase Assays**

Enzyme	Final volume	Substrate	Buffer	pH	Additions
	ml				
Phosphatase	1.0	12.5 mM *p*-nitrophenyl phosphate	0.1 M acetate	5.0	—
α-Galactosidase	0.2	0.1 mM 4-methylumbelliferyl-α-galactopyranoside	0.05 M cacodylate	6.5	—
β-Galactosidase‡	0.5	5 mM *p*-nitrophenyl-β-D-galactopyranoside	0.1 M cacodylate	6.0	2 mM EDTA or 2 mM $MnCl_2$
β-*N*-Acetylgalactosaminidase	0.5	4.4 mM *p*-nitrophenyl-*N*-acetyl-β-D-galactosaminide	0.1 M cacodylate	6.5	—
β-*N*-Acetylglucosaminidase	0.5	4.4 mM *p*-nitrophenyl-*N*-acetyl-β-D-glucosaminide	0.1 M cacodylate	6.5	—
β-Glucuronidase	0.5	5 mM *p*-nitrophenyl-β-glucuronide	0.1 M acetate	5.0	—
Protease	1.3	20 mg denatured hemoglobin§	0.77 M cacodylate	6.5	—

* All incubation mixtures contained Triton X-100 in a final concentration of 0.1% (43).

‡ Assays run separately with one and the other addition served to calculate the activities of β-galactosidase I and II (see text).

§ 2.2 g hemoglobin are dissolved in H_2O with 36 g urea and 8 ml 1 N NaOH in 100 ml total volume. After 30–60 min at room temperature 10 ml 1 M cacodylate buffer pH 6.5 and 4 g urea are added and the pH is adjusted to 6.5 (27).

TABLE II

Analytical Procedures for Hydrolase Assays

Enzyme	Manipulation after incubation	Analysis	Reference
Phosphatase β-Galactosidase β-*N*-Acetylgalactosaminidase β-*N*-Acetylglucosaminidase β-Glucuronidase	Add 3 ml of 133 mM glycine buffer, pH 10.7	Measurement of absorbance at 410 nm of liberated *p*-nitrophenol	(4, 30)
α-Galactosidase	Add 2 ml of above buffer	Measurement of fluorescence of liberated 4-methylumbelliferol (λ_{ex} = 365 nm; λ_{em} = 460 nm)	(33)
Protease	Add 10 ml of 3.5% trichloroacetic acid, centrifuge in cold after 30 min	Automated Lowry assay on supernatant for acid soluble digestion products. Concentration of NaOH increased to compensate for acid in sample	(28, 30)

FIGURE 1 Electron micrograph of *Tritrichomonas foetus*. *Ax*, axostyle; *C*, costa; *ER*, endoplasmic reticulum; *G*, Golgi complex; *Gl*, glycogen; *Lg*, lysosome-like granules; *Mg*, microbody-like granules; *N*, nucleus. × 14,580.

Subcellular particle fractions were fixed similarly with buffered glutaraldehyde, and then collected and washed by filtration under pressure onto Millipore filter disks (Millipore Corp., Bedford, Mass.) with pore sizes of 220 nm (GSWP 01300) or 100 nm (VCWP 01300) according to the method of Baudhuin et al. (6) which gives representative sampling of the material. The disks were folded in half after removal from the apparatus instead of being sandwiched with red blood cells.

The pellets of intact cells and subcellular fractions were postfixed in 1% osmium tetroxide buffered with 100 mM phosphate or 100 mM cacodylate, pH 7.4. The fractions, but not the cells, were stained with uranyl acetate before dehydration. All samples were dehydrated in graded ethanol solutions, cleared in propylene oxide, and embedded in Epon. Thin sections were cut on a Porter-Blum model 2B ultramicrotome, stained with uranyl acetate and lead citrate, and viewed in a Philips EM 300 microscope.

RESULTS

Cytoplasmic Granules of Intact T. foetus

As noted (25, 39), low power electron micrographs reveal many different cytoplasmic structures (Fig. 1). The ground cytoplasm is rich in free ribosomes; there are large clusters of glycogen granules. A wide variety of membrane-limited structures can be observed. In the following we describe in some detail those which were recognized in the different fractions of the fractionation experiments and characterized as to their enzyme content.

The most conspicuous structures are large round bodies, corresponding to the paraxostylar and paracostal granules (chromatic granules) of the light microscopists. They clearly fall into two types. Members of the first type are somewhat smaller than those of the second type and vary

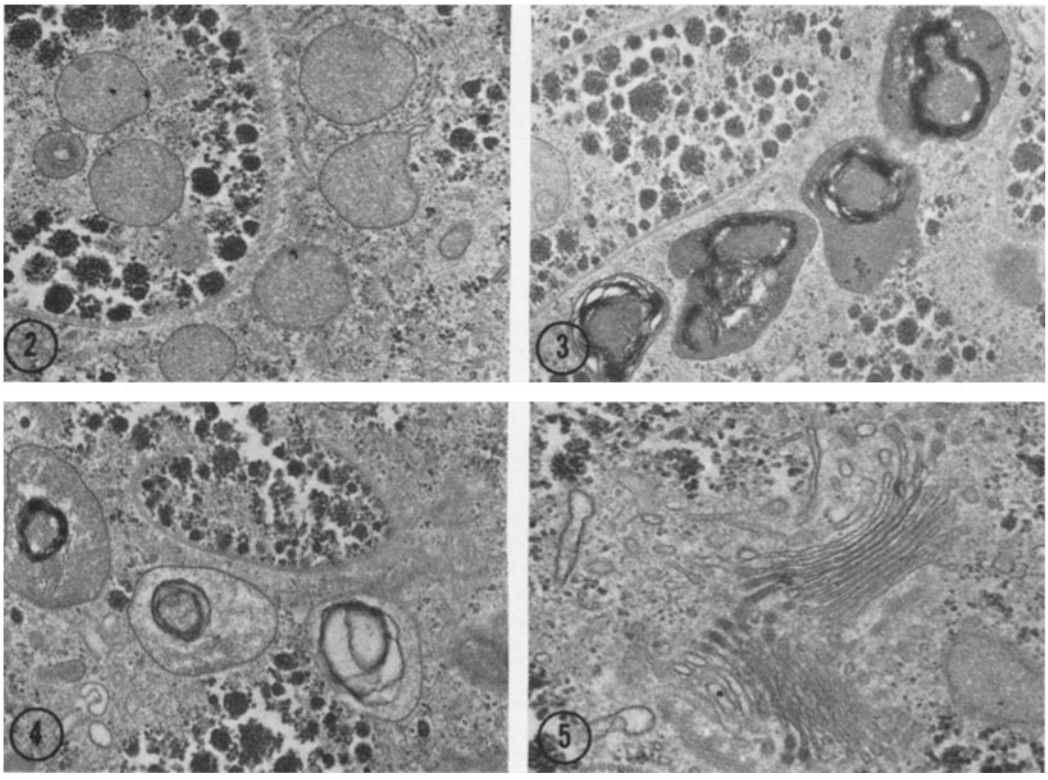

FIGURES 2–5 Electron micrographs of *T. foetus* organelles *in situ*. Fig. 2: Microbody-like granules. × 23,490. Figs. 3 and 4: Lysosome-like granules. × 18,360 and × 21,300. Fig. 5: Golgi complex. × 34,080.

very little in size (Fig. 2). They are more prevalent in the anterior half of the organism and are rarely found in the posterior half. The structures are surrounded by a single membrane and filled with a finely granular matrix. There is often a flattening or depression on one side where the membrane is apparently thicker. In some granules the presence of round internal structures, slightly denser than the matrix, is indicated, usually adjacent to the flattening. Since their morphology is similar to that of microbodies found in other organisms, these granules will be referred to as microbody-like granules.

The other large particle type has a much less defined topography, but seems to be more abundant in the rear half of the body. These granules are somewhat larger than the microbody-like granules and vary in size (Figs. 3 and 4). Their shape is less regular. Elongated structures or protrusions from the main body are quite frequent. The single membrane envelope is conspicuous. The contents of these granules show great variations. The matrix is coarse, and often shows areas of higher density or empty spaces. Myelin figures and pleomorphic inclusions are common. On the basis of their morphology these structures are likely to be the sites of intracellular breakdown of materials, resembling lysosomes in this respect, and will be referred to as lysosome-like granules.

Another very prominent structure is the parabasal apparatus, i.e., Golgi complex with its derivative small vesicles. It is known to be localized in the anterior end of the body in the vicinity of the basis of the locomotor apparatus. The complex does not reveal any unusual features (Fig. 5).

In addition to the above structures there are occasional profiles of rough endoplasmic reticulum, especially around the nucleus, and many vesicles of varying size.

Enzymes

Table III lists the specific activities of the enzymes assayed in homogenates of *T. foetus*. Fig. 6 shows the pH activity curves of some hydrolases for which no data were available in the literature. All three enzymes, especially the protease, are active over a remarkably wide range of pH. Other hydrolases were assayed at their pH optimum as given by Watkins (42). For β-*N*-acetylglucosaminidase we confirmed her data. The malate dehydrogenase assay determines the total NAD-linked activity and does not differentiate between nondecarboxylating and decarboxylating enzymes. Therefore the term malate dehydrogenase will be used to designate the combined activity of these enzymes. Properties of these and the other oxidoreductases listed in Table III will be reported on in a subsequent publication.

Distribution of Marker Enzymes

Differential centrifugation of homogenates of *T. foetus* revealed characteristic distribution patterns for different enzymes or groups of enzymes. In

TABLE III

Specific Activities of Enzymes in T. foetus Homogenates
(mU/mg protein ± SD [number of determinations])

Enzymes	Temperature	Activity
	°C	
NADH dehydrogenase	30	718 ± 248 (5)
NADPH dehydrogenase	30	12.8 (1)
α-Glycerophosphate dehydrogenase	30	10.1 (1)
Malate dehydrogenase	37	91.7 ± 38.7 (6)
Catalase	0	32.3 ± 6.7 (5)
Phosphatase	37	57.2 ± 16.7 (15)
α-Galactosidase	23	1.5 (1)
β-Galactosidase I	23	37.9 (1)
β-Galactosidase II	23	37.2 (1)
β-*N*-Acetylgalactosaminidase	23	62.7 ± 12.6 (3)
β-*N*-Acetylglucosaminidase	23	112 ± 51.2 (17)
β-Glucuronidase	37	6.7 ± 1.3 (3)
Protease	37	181 ± 59.6 (7)

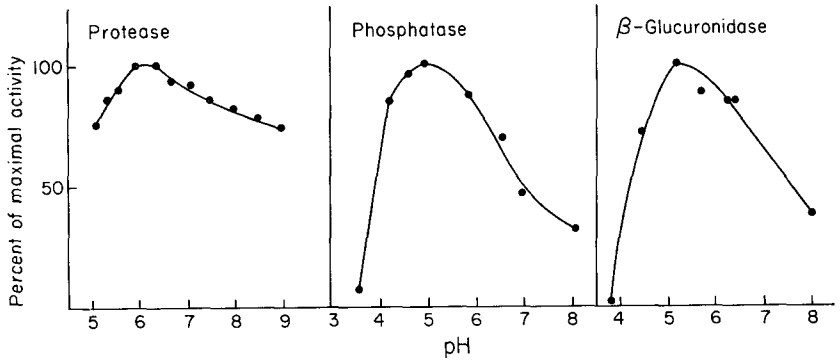

FIGURE 6 Influence of pH on activity on *T. foetus* hydrolases. Assays performed in 0.1 M acetate-cacodylate (phosphatase and β-glucuronidase) or 0.077 M cacodylate-borate (protease) buffers.

Fig. 7 we summarize the results of four such experiments.

The distribution of NADH dehydrogenase, as shown in the left-hand column, is characterized by a large amount of activity in the final supernatant, a practical absence of the enzyme in the intermediate particle fractions and a variable amount in the first, large particle fraction which contains intact cells. This suggests strongly that NADH dehydrogenase is essentially located in the soluble cytoplasm and that the variable amounts of this enzyme recovered in the first fraction reflect that population of unbroken cells in the homogenate. That many of the cells actually fail to rupture under our homogenization conditions and sediment with the first particle fraction was noted by phase-contrast microscopy. But this was accepted as the lesser evil, since otherwise extensive damage to the fragile cytoplasmic components would have occurred. However, the presence of large and variable numbers of intact cells in the preparations tends to obscure the significance of the distribution patterns and to complicate comparison between experiments.

To circumvent this difficulty, we have assumed that the proportion of NADH dehydrogenase contained in the first fraction is a measure of the proportion of unbroken cells in the homogenate. On this assumption, we have in each experiment subtracted from protein and enzyme percentage values characteristic of the first fraction an amount equal to percentage content of this fraction in NADH dehydrogenase, and normalized the remainder of this distribution pattern, which is now known to apply to the components of broken cells only. The validity of this procedure is supported by comparison of the corrected (second column of Fig. 7) with the uncorrected (first column of Fig. 7) distribution of NADH dehydrogenase. The corrected amount of protein associated with the final supernatant lies between 35 and 40% of the total in all four experiments, whereas the uncorrected values vary from 23 to 35%. All other distributions in Fig. 7 have been similarly treated.

Looking now at the correlated results of experiment no. 1, we see that the other three enzymes assayed besides NADH dehydrogenase are all associated almost entirely with sedimentable components, but that each shows a distinctive distribution pattern. Malate dehydrogenase is concentrated largely in fraction II, where it shows a sixfold increase in specific activity.

In contrast, β-*N*-acetylglucosaminidase and phosphatase are distributed over several fractions. The former is present in fractions containing large particles sedimenting with low centrifugal forces, whereas the latter, though also present in these fractions, reaches its highest specific activity in fractions containing smaller particles and practically devoid of β-*N*-acetylglucosaminidase.

Not included in this experiment was catalase, which is to a very large extent soluble. However, about 10% of its activity is consistently connected with fractions containing large particles. This is clearly shown in the lower rows of Fig. 7 (exp. no. 2–4).

On this basis, we can tentatively conclude that there are at least three different particle populations present in *T. foetus*. A large particle population of fairly uniform sedimentation properties contains malate dehydrogenase. Another group of large particles, more heterogeneous in size and including some very large representatives, carries the neutral β-*N*-acetylglucosaminidase and part

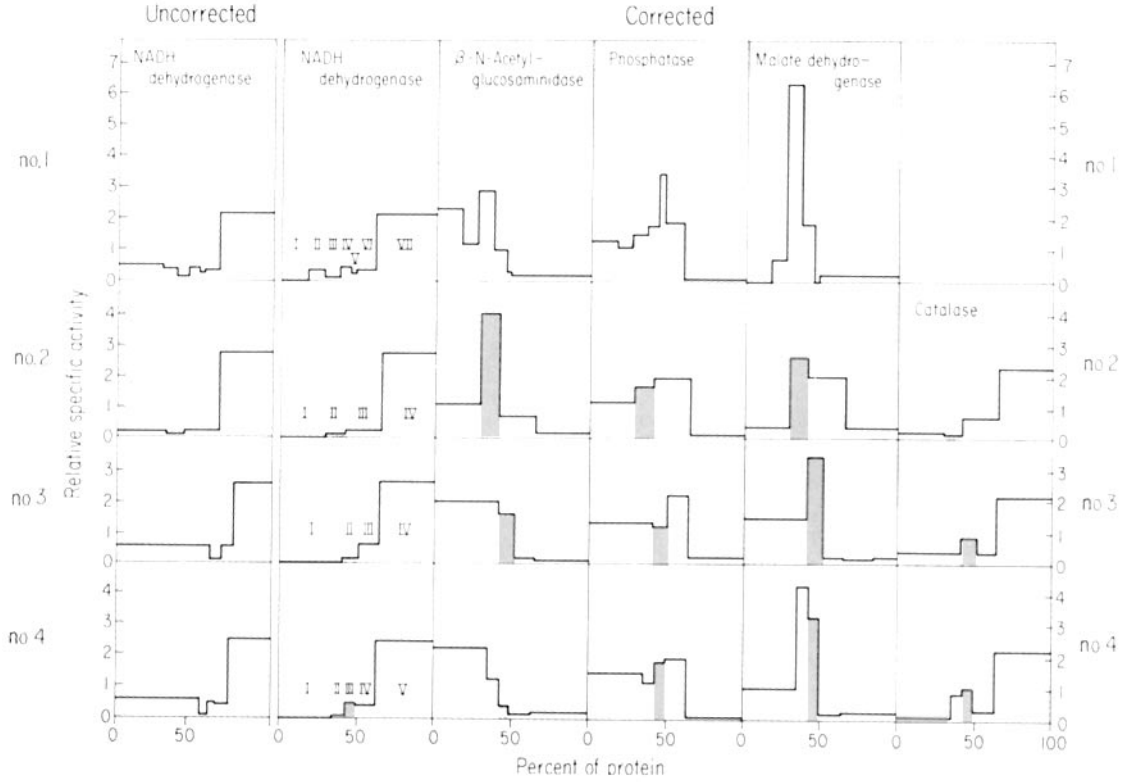

FIGURE 7 Distribution of marker enzymes after differential centrifugation of *T. foetus* homogenates. Relative specific activity of the enzymes plotted against cumulative percent of protein recovered in each fraction. In each graph the direction from left to right corresponds to increasing centrifugal fields. The far right-hand block represents the final supernatant. Left-hand column gives original data; all other columns were corrected for the amount of unbroken cells in homogenate (see text). Distribution of additional enzymes shown in Figs. 9–11. Areas shaded in exp. no. 2–4 designate the fractions subjected to isopycnic centrifugation (Figs. 8–11). Centrifugation conditions are given in Table IV, percentage recoveries in Table V.

of the acid phosphatase. A small particle population has the rest of the phosphatase. The localization of the sedimentable portion of catalase is less clear, but does not seem to correspond to any of the above three populations.

Based on these results, simplified fractionation schemes were used to prepare particulate fractions specifically enriched in one or the other major particle population, for further subfractionation by isopycnic centrifugation. The observed distributions are presented in the second through fourth rows of Fig. 7. They clearly confirm the results of experiment no. 1. The stippled parts of the diagrams in Fig. 7 indicate the fractions that were used for further subfractionation by isopycnic centrifugation, to give the results shown in Fig. 8. For clearer appreciation, the surface areas of the density distribution diagrams in Fig. 8 have been made proportional to the percentage of total enzyme activity associated with the fraction used as starting material (shaded area in Fig. 7), with the ordinate scale expanded threefold for catalase and protein.

In considering the results of Fig. 8, we may disregard the secondary dense peaks shown by all components, especially protein, in experiment no. 2; they reflect obvious agglutination artifact, presumably caused by the presence of large numbers of nuclei in the starting material.

Particularly striking is the distribution profile of malate dehydrogenase, which in all three experiments bands in a narrow zone with a modal density of 1.24. This part of the gradient contains

very little hydrolase activity but there is some overlap with the distribution of catalase.

The small amount of catalase activity in the initial particle fractions does not remain in the sample zone but migrates into the gradient and forms a narrow zone around a density of 1.22. Although there is some overlap with the distribution of other enzymes, this peak is clearly different

TABLE IV

Conditions of Differential Centrifugation
(Figs. 7 and 9–11)

Fraction	Experiment no. 1		Experiment no. 2		Experiment no. 3		Experiment no. 4	
	min	*rpm* (*g*)	*min*	*rpm* (*g*)	*min*	*rpm* (*g*)	*min*	*rpm* (*g*)
I	4	1,000 (87)	6	1,000 (87)	4	2,500 (546)	5	2,000 (350)
II	3	2,400 (504)	10	4,000 (1,400)	10	7,500 (4,920)	10	5,500 (2,650)
III	10	4,000 (1,400)	30	39,000* (105,000)	30	19,000* (31,500)	10	10,000 (8,750)
IV	10	7,000 (4,300)					30	39,000* (109,000)
V	10	10,000 (8,750)						
VI	30	39,000* (109,000)						

Centrifugation done in a Sorvall RC-2B refrigerated centrifuge equipped with an SM-24 rotor, except the 39,000 rpm step, which was done in a Spinco HL preparative ultracentrifuge with a no. 40 rotor (Beckman Instruments, Inc., Spinco Div., Palo Alto, Calif.). Tubes of 3.5 ml capacity (Sorvall no. 250) and the corresponding adaptors (Sorvall no. 314) (R_{min}, 6.4 cm; R_{max}, 9.2 cm) were used in the Sorvall centrifuge and tubes of 2 ml capacity (Beckman no. 303369) and adaptors (Beckman no. 303376) (R_{min}, 5.3 cm; R_{max}, 7.8 cm) were used in the Spinco centrifuge. The *g* values refer to the center of the tube. All sediments were washed once and the two supernatants combined, except those marked with an asterisk which remained unwashed.

TABLE V

Percent Recoveries in the Fractionation Experiments
(Figs. 7–11)

Enzyme	Differential centrifugation*				Isopycnic centrifugation‡		
	Exp. no. 1	Exp. no. 2	Exp. no. 3	Exp. no. 4	Exp. no. 2	Exp. no. 3	Exp. no. 4
β-*N*-Acetylglucosaminidase	87	105	85	78	75	108	89
β-*N*-Acetylgalactosaminidase	—	94	—	—	132	—	—
β-Galactosidase II	—	67	—	—	90	—	—
Protease	—	89	—	—	92	—	—
Phosphatase	95	136	120	97	99	125	104
β-Glucuronidase	—	—	—	87	—	—	108
α-Glycerophosphate dehydrogenase	—	—	98	—	—	106	—
Malate dehydrogenase	110	125	100	57	125	91	74
Catalase	—	85	91	92	126	76	47
NADH dehydrogenase	76	108	117	117	—	—	—
Protein	91	112	100	103	92	97	94

* As compared with whole homogenate.

‡ As compared with initial particle fraction.

from that of malate dehydrogenase, showing that catalase is not associated with the dehydrogenase-carrying structures.

In contrast with the preceding enzymes the hydrolases show density distributions that are not independent of the sedimentation coefficients of their host particles. The distribution of β-*N*-acetylglucosaminidase, although monomodal in

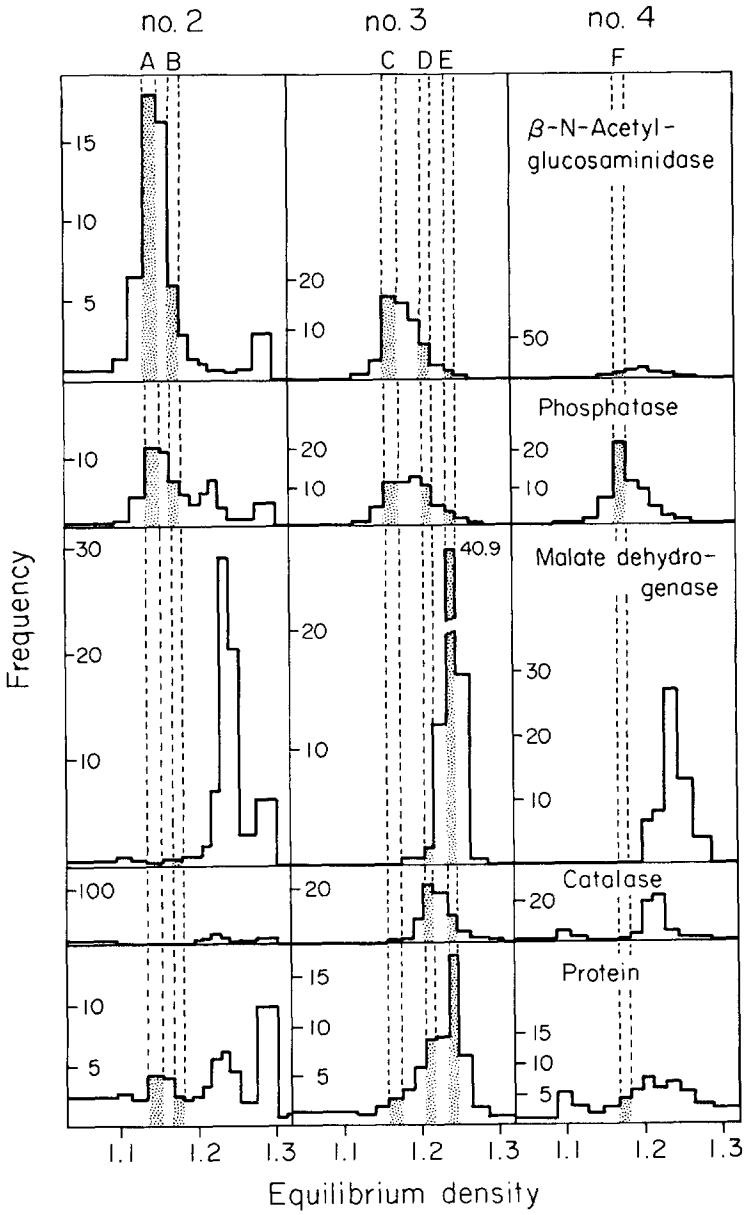

FIGURE 8 Distribution of marker enzymes after isopycnic centrifugation of *T. foetus* particle fractions (see Fig. 7). Density frequency plots. The area under each histogram is proportional to the percentage of total enzyme activity present in the fraction used as starting material. The ordinate has been expanded threefold for catalase and protein, to improve clarity. Fractions A–F are those of which electron micrographs are shown in Figs. 15–20. Distribution of additional enzymes shown in Figs. 9–11. Percentage recoveries are given in Table V.

appearance, clearly shifts progressively from a modal density of about 1.15 in the more rapidly sedimenting part of the population (exp. no. 2) to one of 1.20 in the more slowly sedimenting part (exp. no. 4). Apparently, therefore, decreasing size correlates with increasing equilibrium density in this population.

Distribution of phosphatase also varies from gradient to gradient. In experiments no. 2 and 3 its distribution is fairly close to that of β-*N*-acetyl-

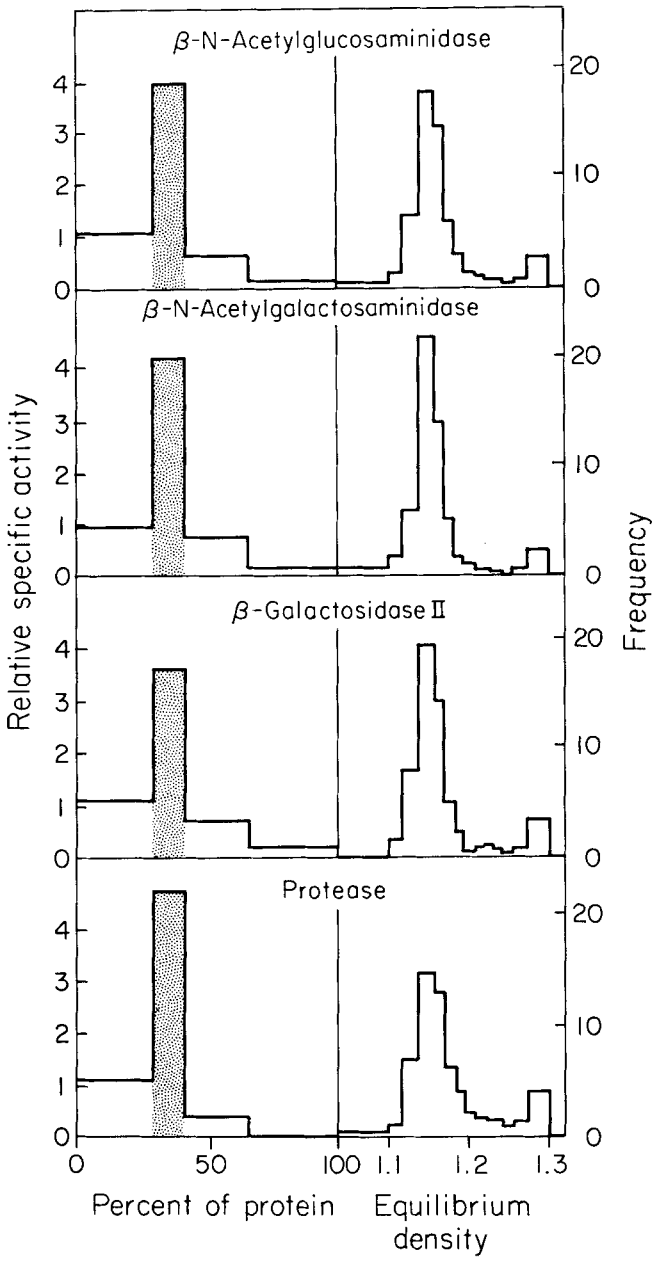

FIGURE 9 Distribution of neutral hydrolases in a differential (left) and isopycnic (right) centrifugation experiment (No. 2). Presentation as in Figs. 7 and 8, but the density-frequency plots were not adjusted for the enzyme activity of the starting material. Additional data in Tables IV and V.

glucosaminidase. The little secondary peak on the denser side in experiment no. 2 has been seen only in this single gradient and has to remain unexplained. In contrast, the distribution of phosphatase is quite different from that of β-*N*-acetylglucosaminidase in the gradient on small particles (exp. no. 4), forming a fairly symmetrical profile around a density of 1.18, clearly representative of the second group of acid phosphatase-containing particles revealed by the differential centrifugation experiments.

The distributions of protein are expectedly different in the three gradients. Compared with the enzyme distributions, they indicate that the bulk of the protein in the three fractions belongs to the granules containing malate dehydrogenase and β-*N*-acetylglucosaminidase, and that the small particles carrying phosphatase represent only a minor contribution to the total protein.

Distribution of Additional Enzymes

In addition to the major marker enzymes for the different subcellular components, we studied the distribution of several other enzymes. The distribution of β-*N*-acetylglucosaminidase is followed by three other neutral hydrolases, β-*N*-acetylgalactosaminidase, β-galactosidase II, and protease (Fig. 9). α-Glycerophosphate dehydrogenase and malate dehydrogenase show identical patterns (Fig. 10). Phosphatase and β-glucuronidase are distributed similarly in differential centrifugation, with β-glucuronidase consistently having lower activity in the larger granule fractions. There is no difference in their isopycnic distribution as determined on a small particle fraction (Fig. 11). Over 90% of the activity of NADPH dehydrogenase, of α-galactosidase, and of β-galactosidase I, was in the final supernatants, showing that, like NADH-dehydrogenase, these enzymes are in the nonsedimentable portion of the cytoplasm.

Latency Studies

In Fig. 12 are shown the results of some latency studies on malate dehydrogenase in a particle fraction. If the assay was performed without osmotic protection, a high activity was registered and injection of the nonionic detergent Triton X-100 into the chamber (final concentration 0.1%)

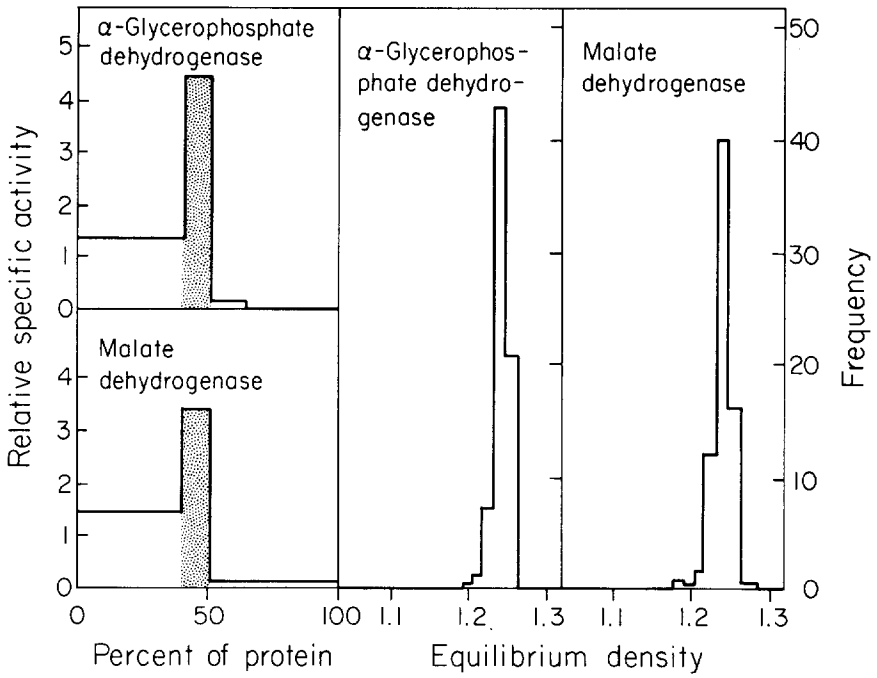

FIGURE 10 Distribution of dehydrogenases in a differential (left) and isopycnic (right) centrifugation experiment (no. 3). Presentation as in Figs. 7 and 8, but the density-frequency plots were not adjusted for the enzyme activity of the starting material. Additional data in Tables IV and V.

did not cause any marked increase in the rate (Fig. 12 A). However, if the particles were osmotically protected by 0.25 M sucrose, the reaction rate was very low, indicating the existence of a permeability barrier between the exogenous substrates (NAD or malate) and the enzyme (Fig. 12 B). This barrier can be suppressed by Triton X-100 (0.1% final concentration) or by four cycles of freezing

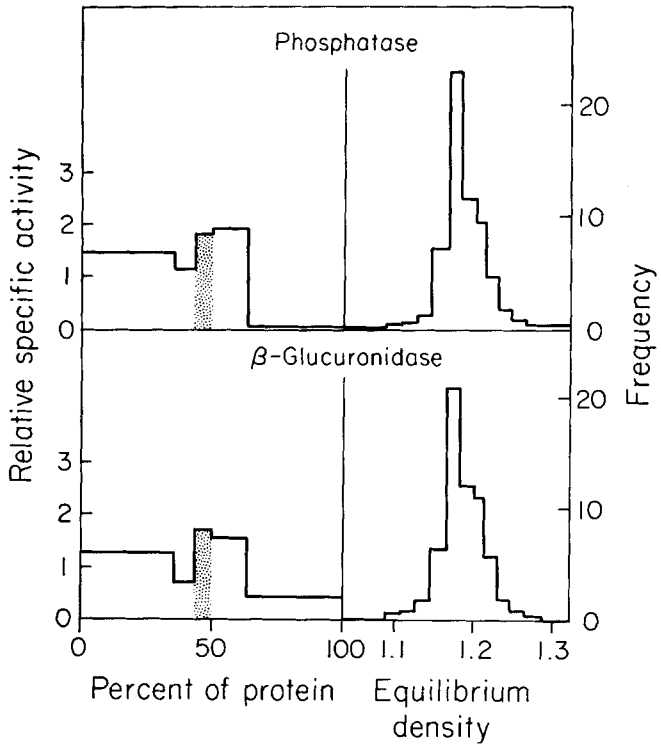

FIGURE 11 Distribution of acid hydrolases in a differential (left) and isopycnic (right) centrifugation experiment (No. 4). Presentation as in Figs. 7 and 8, but the density-frequency plots were not adjusted for the enzyme activity of the starting material. Additional data in Tables IV and V.

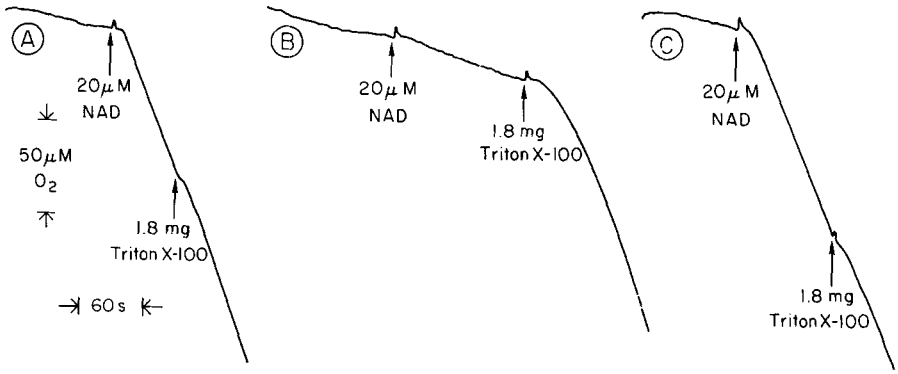

FIGURE 12 Polarographic measurement of malate dehydrogenase activity in a large particle fraction of *T. foetus*. Assay performed as described in Methods, but at 26°C. The particle fraction was a fraction sedimented for 10 min at 5,500 rpm from the supernatant of a 4 min centrifugation at 2,000 rpm and it contained 42.6% of the malate dehydrogenase activity and 9.6% of the total protein of the homogenate. (A) Assay performed in the absence of sucrose, (B, C) assays in the presence of 0.25 M sucrose on intact (B) and frozen and thawed particles (C).

and thawing (Fig. 12 C). These results suggest that malate dehydrogenase is contained in a membrane-bounded particle sensitive to hyposmotic conditions, freezing and thawing, or detergent action and that in the homogenate the dehydrogenase particles or their membranes are not damaged.

The hydrolases are also largely latent in preparations osmotically protected with 0.25 M sucrose, and are released by Triton X-100 (Fig. 13). Repeated freezing and thawing, however, activated fully only the neutral hydrolases. In contrast, this treatment has only a slight effect on β-glucuronidase. It causes partial release of acid phosphatase in a mixed particle fraction (Fig. 13), but frees this enzyme completely in a fraction consisting predominantly of large particles (Fig. 14). These results suggest that the large particles carrying the neutral hydrolases and part of the phosphatase are very sensitive to freezing and thawing, whereas the small particles containing the rest of the phosphatase and most of the β-glucuronidase are much more resistant to such treatment.

Morphology of the Subcellular Fractions

All the fractions described above were examined in the electron microscope. We illustrate here only those in which particularly high specific activities were attained fairly selectively for a certain set of enzymes (Table VI).

Fig. 15 shows the appearance of fraction E, which appears biochemically (see Table VI and Fig. 8) as a fairly pure preparation of the large granules containing the dehydrogenases. The dominant structures are round (or flattened due to the pressure during filtration), membrane-limited granules of fairly large size with a uniform granular matrix. These structures contain occasionally one or two membrane-limited smaller inclusions but never resemble the lysosome-like granules. Although they appear somewhat less

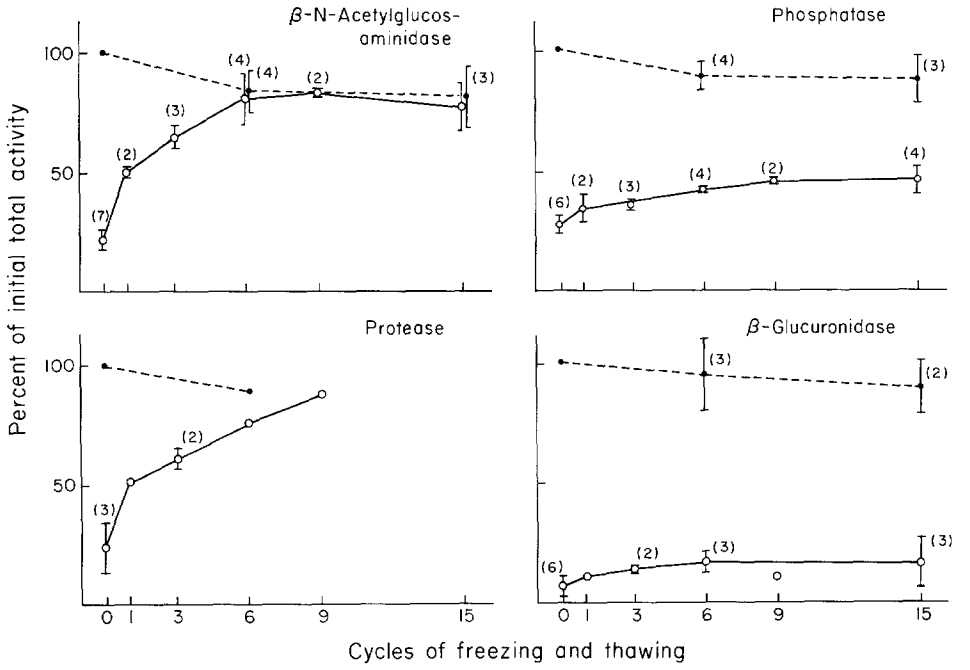

FIGURE 13 Effect of freezing and thawing on the total (broken lines) and free (solid lines) activity of hydrolases in *T. foetus* homogenates. Bars through the experimental points give SD. Number of experiments in parentheses. Assays at 23°C for 30 min in the presence of 0.25 M sucrose for free and in the presence of 0.25 M sucrose and 0.1% Triton X-100 for total activity. The preparations were homogenates cleared of intact cells and from debris by centrifugation for 4 min at 2,000 rpm (350 *g*); they contained (mean ± SD) 63.1 ± 8.6% (7) of protein, 43.5 ± 16.1% (7) of β-*N*-acetylglucosaminidase, 44.4 ± 11.2% (2) of protease, 57.8 ± 5.2% (6) of phosphatase, and 67.4 ± 9.9% (5) of β-glucuronidase of the original homogenate.

dense than their counterparts in intact cells, their identity with the microbody-like structures is clear. These structures can be found only in fractions containing dehydrogenases and thus they can be identified unequivocally as the subcellular sites of these enzymes.

Fig. 16 shows the catalase-rich fraction D. Biochemically this fraction is contaminated by only small amounts of particles carrying dehydrogenases and hydrolases, which together cannot make up more than 15–20% of its total protein content. However, the degree of purity of the catalase-containing particles is impossible to assess without information on the significance of the soluble catalase. If this enzyme originates from broken particles, the purity of the fraction is bound to be low. If none of it comes from broken particles, the purification could be as high as 20-fold, a value compatible with a fairly high degree of purity, though by no means demonstrative of it. The morphology confirms the low degree of contamination by large granules, but reveals a complex composition. There are large numbers of round or elongated small bodies, flagella, as well as other unidentified structures which could be the site of location of particulate catalase.

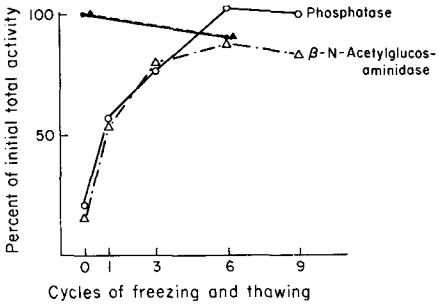

FIGURE 14 Effect of freezing and thawing on the free (open symbols) and total (solid symbols) activity of hydrolases in a large cytoplasmic particle fraction of *T. foetus*. Assay conditions as in Fig. 11. The particle fraction was separated from the supernatant of a 4 min centrifugation at 2,000 rpm by centrifugation for 10 min at 5,000 rpm (2650 *g*); it contained 13.1% of protein, 22.7% of phosphatase, and 32.1% of β-*N*-acetylglucosaminidase of the whole homogenate.

Fig. 17 depicts the appearance of fraction A which is our purest preparation of the large granules of low density, characterized biochemically by their content of neutral hydrolases. The most conspicuous components of this fraction are recognized as large granules with internal myelin figures and partially disrupted or depleted matrix. In addition there are a few particles, obviously of the same family but with a tighter matrix, and much debris which appears to originate from damaged particles of the same group. Fraction B, which is a biochemically less pure preparation of hydrolase-containing granules separated at a higher density, resembles fraction A in appearance (Fig. 18). The granules in this fraction tend to be more densely filled than those in fraction A, and the fraction contains a much larger proportion of amorphous material. A few flattened vesicles similar to those seen in fraction F (see below) are also visible. These findings, added to the centrifugal behavior of the neutral hydrolases, clearly identify the very large heterogeneous, lysosome-like granules as the bearers of these enzymes.

Fig. 19 shows the appearance of the acid

TABLE VI

Enzymatic Composition of Fractions, Whose Ultrastructure Is Shown in Figs. 15–20*
(R.S.A. of homogenate = 1)

Enzyme	Fraction					
	A	B	C	D	E	F
α-Glycerophosphate dehydrogenase	—	—	0.0	0.50	**10.89**	—
Malate dehydrogenase	0.10	0.43	0.14	0.55	**8.07**	0.0
Catalase	0.0	0.04	0.16	**2.00**	0.45	0.31
β-*N*-Acetylglucosaminidase	**16.94**	**9.74**	**9.48**	1.22	0.13	0.63
β-*N*-Acetylgalactosaminidase	**21.87**	**8.97**	—	—	—	—
β-Galactosidase II	**16.92**	**7.29**	—	—	—	—
Proteinase	**16.81**	**12.10**	**8.08**	1.69	0.25	0.52
Phosphatase	**4.63**	**4.53**	**5.03**	1.35	0.23	**10.41**
β-Glucuronidase	—	—	—	—	—	**8.98**

* As relative specific activities (R.S.A.).

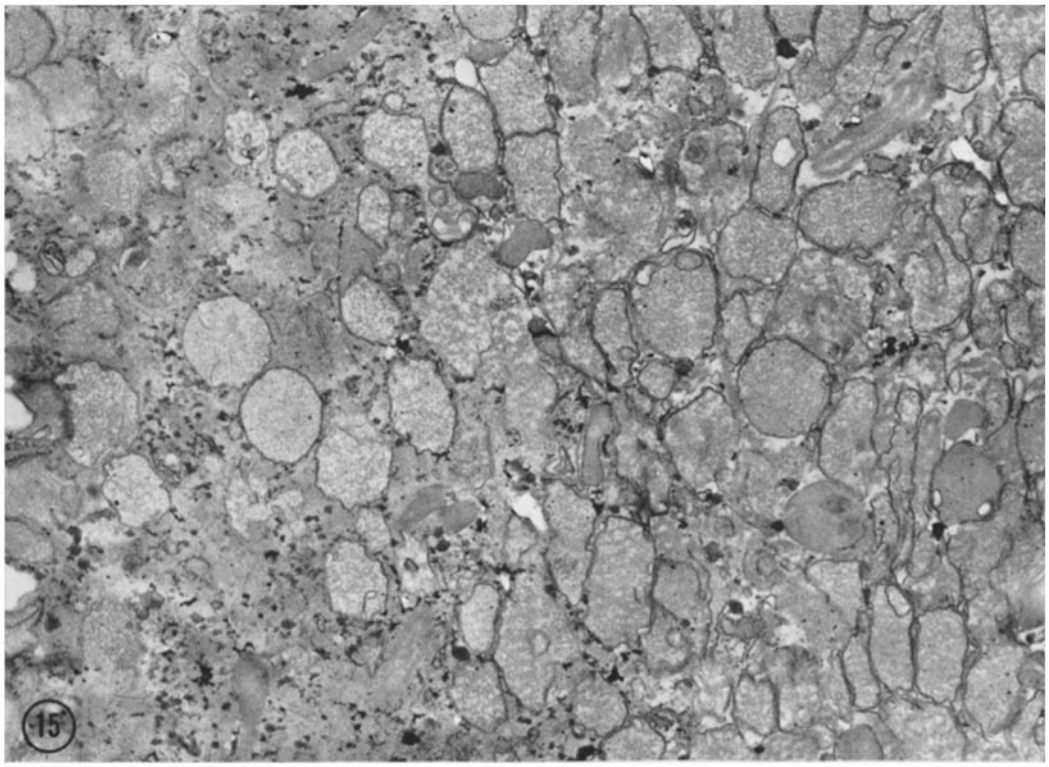

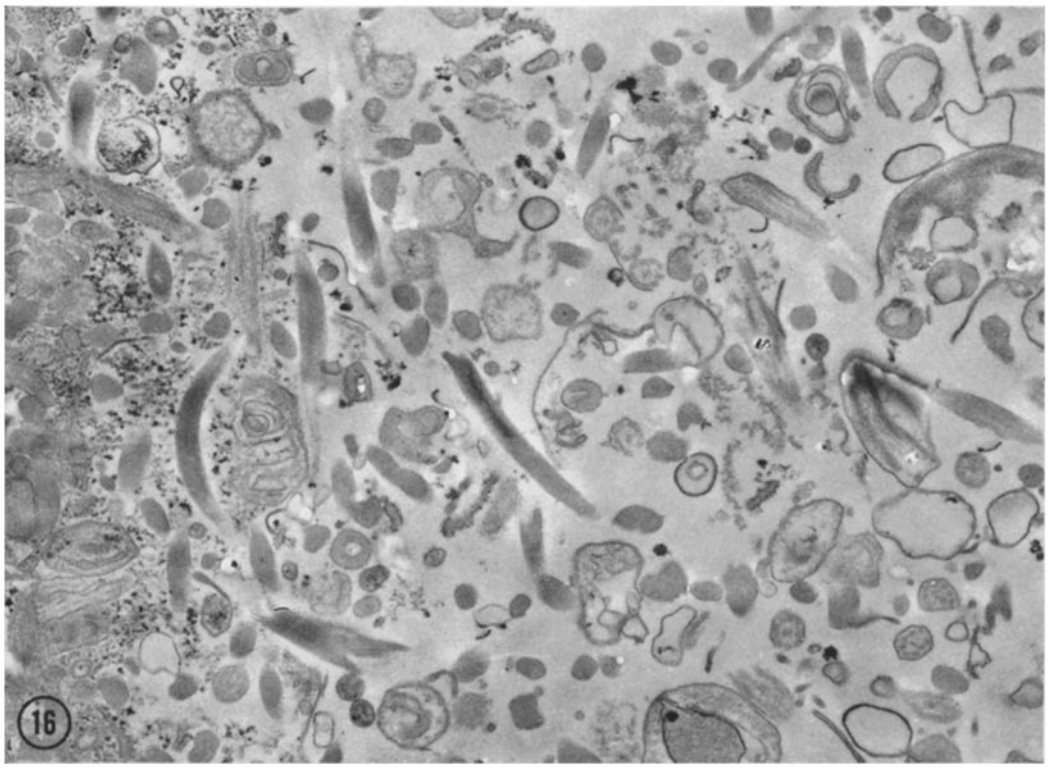

FIGURES 15–20 Electron micrographs of fractions obtained by isopycnic centrifugation and described in Table VI. Areas shown correspond to more than $^{9}/_{10}$ of total thickness of the pellets. Bottom of pellet is on the left, top on the right. × 22,145.

FIGURE 15 Dehydrogenase-rich fraction E (exp. no. 3, $\rho = 1.242$).

FIGURE 16 Catalase-rich fraction D (exp. no. 3, $\rho = 1.211$).

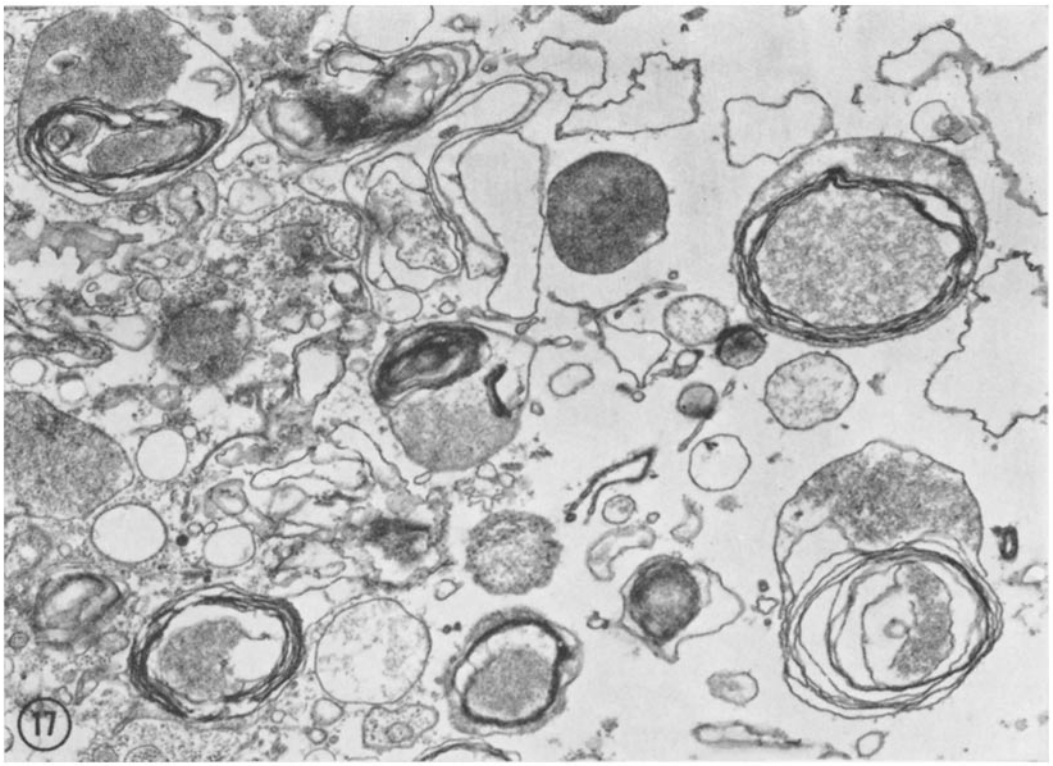

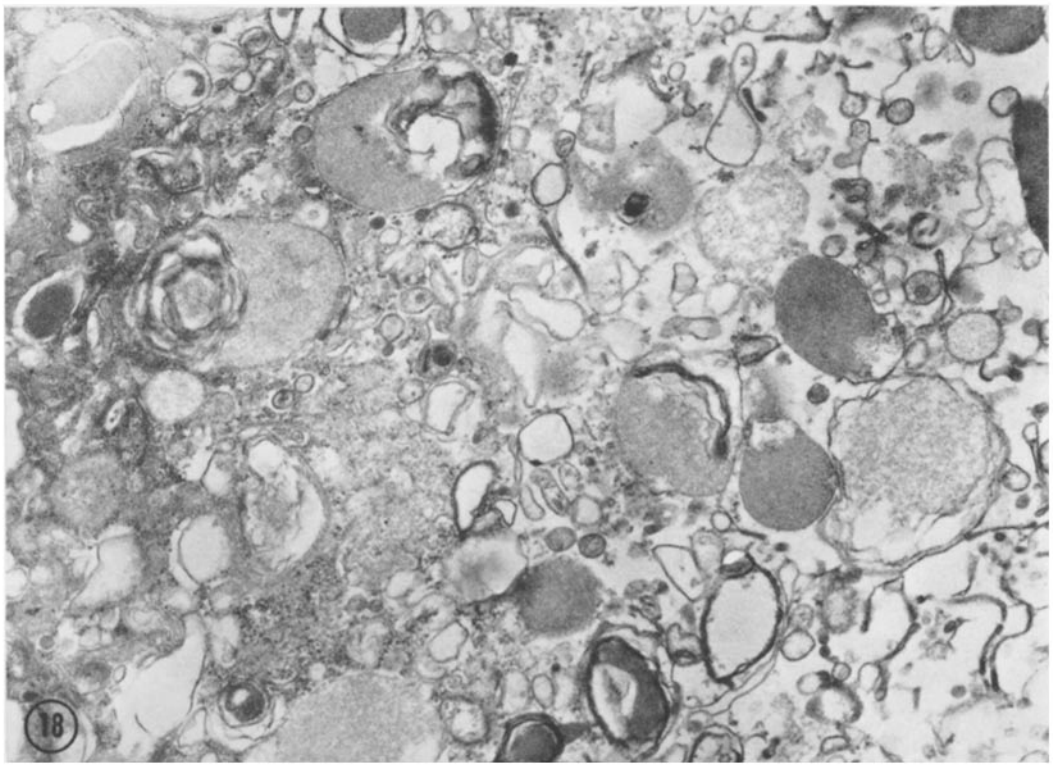

FIGURES 17 and 18 Neutral hydrolase-rich fractions A and B (exp. no. 2, ρ = 1.148 and 1.176).

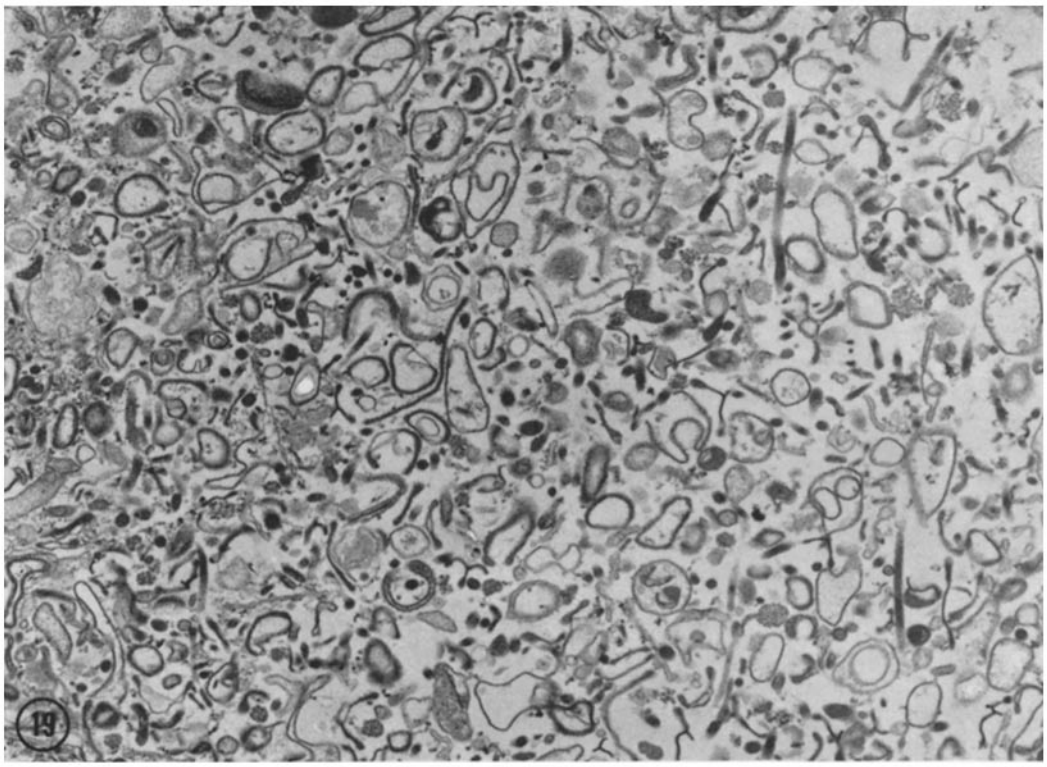

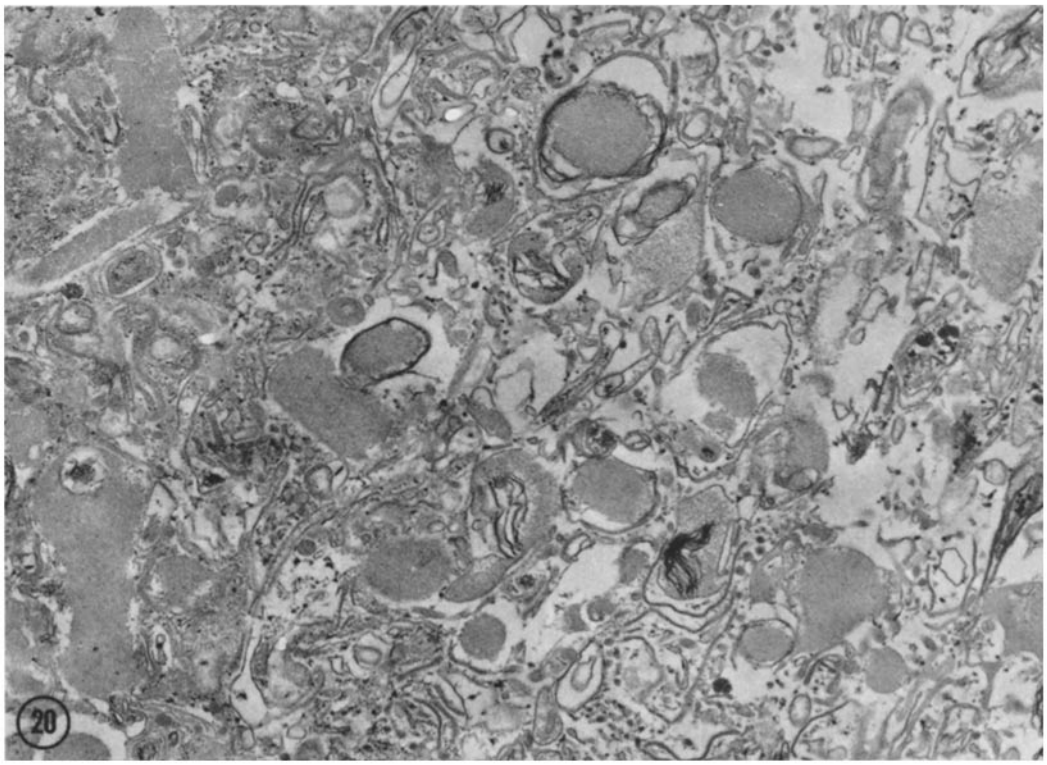

FIGURE 19 Acid hydrolase-rich fraction F (exp. no. 4, $\rho = 1.175$).

FIGURE 20 Fraction C containing neutral and acid hydrolases (exp. no. 3, $\rho = 1.166$).

hydrolase-rich fraction F. This fraction contains only very few larger structures and consists mostly of small dense granules, often rounded, often elongated, frequently with swellings at the ends. On the basis of their morphology these are very likely derivatives of Golgi complex. Another frequent element of the picture is represented by less dense, small, round, or flattened vesicles. At the present moment the relationship of the two elements is unclear, just as it is difficult to determine if both groups or only one of them carries the acid hydrolases.

Fig. 20 shows the appearance of fraction C. In agreement with its mode of preparation and biochemical composition, this fraction appears as morphologically intermediate between the hydrolase-rich subfractions separated from rapidly and slowly sedimenting fractions. The granular, and myelin figure containing elements are smaller and less frequent than in fractions A and B, whereas there is a large number of elongated membranous structures similar to those seen in fraction F. At certain points the latter elements are stacked and clearly derived from the Golgi apparatus.

DISCUSSION

In the present work we were able to establish the subcellular localization of some 10 hydrolases and oxidoreductases in *T. foetus* and to identify the organelles that carry the particle-bound enzymes. The findings are summarized in Table VII and will be discussed below.

Localization of Oxidoreductases

The particulate nature of malate dehydrogenase in *Trichomonas vaginalis* has been noted (41), and recently in agreement with our findings, this enzyme was found to be associated with the microbody-like chromatic granules (9).

Catalase is present mainly in the soluble fraction of *T. foetus* homogenates. A small part of the enzyme is connected with particles different from the microbody-like particles. The latter particles cannot be regarded as the source of the soluble catalase

TABLE VII

Characterization of Different Subcellular Components of T. foetus

Subcellular component	Morphology	Equilibrium density in sucrose gradients	Enzymes
Microbody-like granule	Fairly uniform size around 500 nm, uniformly granular matrix surrounded by single membrane, microbody-like. Identification certain.	1.24	α-Glycerophosphate dehydrogenase Malate dehydrogenase
?	?	1.21	Catalase (small part)
Lysosome-like granules	Varying size up to 2 μm, pleomorphic contents often with myelin figures. Identification certain.	1.15–1.20	β-*N*-Acetylglucosaminidase β-*N*-Acetylgalactosaminidase β-Galactosidase II Protease Phosphatase (in part)
Golgi complex	Flattened membranes and smaller (less than 200 nm) vesicles and granules, sometimes in typical Golgi arrangement. Identification probable.	1.18	β-Glucuronidase Phosphatase (in part)
Nonsedimentable cytoplasm	—	—	NADH dehydrogenase NADPH dehydrogenase Catalase (main location) α-Galactosidase β-Galactosidase I

in the cytosol since the integrity of their membrane revealed by the latency of malate dehydrogenase makes it very unlikely that enzymes may have been lost from the particles through leakage. On the other hand, the morphological complexity of the particulate fractions containing catalase does not permit the identification of the particles with which this enzyme is associated. At present, it is impossible to determine whether catalase is entirely located in the cytosol and becomes partly absorbed after homogenization to particulate components, e.g. flagellar structures, that equilibrate at a density of 1.21, or, alternatively, belongs to a very fragile particle of the same density, or, finally has two distinct localizations in the cell.

NADH and NADPH dehydrogenase activity is clearly connected with the soluble cytoplasm and cannot originate from the microbody-like bodies. These findings are in agreement with recent reports on NADH oxidase in *T. vaginalis* (41) and in *T. foetus* (11).

Various suggestions have been made with respect to the possible relationships of the trichomonad microbody-like particles to either mitochondria or peroxisomes (2, 13, 14, 16, 20, 21, 24). So far, these assumptions have been tested with histochemical techniques only (13, 14, 35, 36), and the present study is the first, to our knowledge, to allow a more rigorous discussion of the question in terms of presence and absence of enzymes, at least in *T. foetus*.

Kinship of the microbody-like granules with peroxisomes is suggested by their appearance and consistent with their content in malate dehydrogenase, which is a component of certain plant peroxisomes (44). The hypothesis appears particularly attractive since the organism is devoid of mitochondria and could, in line with de Duve's suggestion (17), use peroxisomes as principal respiratory particle. However, the localization of catalase and our failure so far to detect oxidases in these particles rule out their identification as peroxisomes.

The alternative hypothesis that the particles represent degenerate mitochondria hardly deserves consideration, since it implies such a degree of biochemical and morphological transformation as to make the kinship unrecognizable. It would seem to us more likely that the microbody-like granules of *T. foetus* represent a special type of cytoplasmic bodies which participate in oxidation-reduction reactions, but are different from mitochondria and peroxisomes.

Bodies of similar appearance are permanent structural elements of the mitochondria-free trichomonads (9, 16, 20, 25, 32, 39, 40) and hypermastiginids (24) and of the mitochondria-free holotrich ciliates of the rumen (2, 3, 22). Except for the present study the enzymatic equipment of these bodies is unknown. Obviously, much comparative biochemical work will be needed to ascertain the distribution, in other groups, of organelles similar to the microbody-like particles of *T. foetus*.

Distribution of Hydrolases

It is clear from our data that, in *T. foetus*, hydrolases are located at three distinct sites in the cell. The first of these is represented by the large granules that contain a set of neutral hydrolases. The enzymatic content and the structure of these particles strongly support the idea that they are digestive organelles, comparable in many respects with the lysosomes found in other cell types. However, they differ from typical lysosomes in that several of their enzymes have a pH optimum close to neutrality and are highly active even above pH 7. On the other hand, they contain acid phosphatase and it must be remembered that some lysosomal enzymes have a neutral pH optimum. It seems therefore that we are dealing here with a system very similar if not identical with the lysosomes of other organisms, but which became modified during evolution. The origin of the material digested in this system is unknown.

The second site is occupied by part of the acid phosphatase and most of the β-glucuronidase and seems to be related to the Golgi complex. This idea is supported by electron microscopic histochemical studies which demonstrated acid phosphatase activity in the Golgi complex of *T. foetus* (29) and *T. vaginalis* (8). The possible functional role of the acid hydrolases in the Golgi apparatus and in the derived small vesicles, as well as the relationship, if any, between these and the large digestive structures remains unclear. The third location is the soluble cytoplasm, where several hydrolases, again with unknown function, are present.

The existence of lysosomes in trichomonads has been repeatedly inferred from histochemical observations on granular staining of hydrolases (8, 36, 37) and from the sedimentability and latency of acid phosphatase and hyaluronidase (1, 12, 29). In view of the complex picture of the distribution

of hydrolases in *T. foetus*, further comparative studies are needed to understand the function of the different cytoplasmic sites of hydrolase activity.

The author expresses his thanks to Dr. Bronislaw M. Honigberg (Amherst, Mass.) for the *T. foetus* strain and stimulating discussions, to Dr. Christian de Duve for his great interest and helpful suggestions, to Dr. Marilyn Farquhar for her help with the technical problems of electron microscopy and with the interpretation of the morphological results, to Ms. Cynthia Ward for conscientious technical asssitance, to Ms. Helen Shio for the excellent electron micrography, to Mr. Fred Davidson for performing the calculations on the computer, to Mr. Armando Pelaschier for keeping the equipment in excellent working condition, and, last but not least, to Ms. Anne McDermott and Ms. Jean Smarz for their work on the manuscript.

This work was supported by grant no. GB-5796GX from the National Science Foundation.

Results of this investigation were presented at the 25th Annual Meeting of the Society of Protozoologists (August, 1972 [31]) and the 47th Annual Meeting of the American Society of Parasitologists (November, 1972).

Received for publication 21 September 1972, and in revised form 17 November 1972.

REFERENCES

1. ALCAMO, I. E. 1971. Hyaluronidase production by the trichomonads and the lysosomes of *Tritrichomonas augusta* TAH-CW. Ph.D. Thesis. St. John's University, Jamaica, New York.
2. ANDERSON, E. 1967. Cytoplasmic organelles and inclusions of protozoa. *In* Research in Protozoology. T.-T. Chen, editor. Pergamon Press Ltd., Oxford. **1**:1.
3. ANDERSON, E., and J. N. DUMONT. 1966. A comparative study of the concrement vacuole of certain endocommensal ciliates—a so-called mechanoreceptor. *J. Ultrastruct. Res.* **15**:414.
4. ARONSON, N. N., JR., and C. DE DUVE. 1968. Digestive activity of lysosomes. II. The digestion of the macromolecular carbohydrates by extracts of rat liver lysosomes. *J. Biol. Chem.* **243**:4564.
5. BAUDHUIN, P., H. BEAUFAY, Y. RAHMAN-LI, O. Z. SELLINGER, R. WATTIAUX, P. JACQUES, and C. DE DUVE. 1964. Tissue fractionation studies. 17. Intracellular distribution of monoamine oxidase, aspartate aminotransferase, alanine aminotransferase, D-amino acid oxidase and catalase in rat-liver tissue. *Biochem. J.* **92**:179.
6. BAUDHUIN, P., P. EVRARD, and J. BERTHET. 1967. Electron microscopic examination of subcellular fractions. I. The preparation of representative samples from suspensions of particles. *J. Cell Biol.* **32**:181.
7. BEAUFAY, H. 1966. La centrifugation en gradient de densité. These d'Agrégation de l'Enseignement Supérieur. Université Catholique de Louvain, Louvain, Belgium. Ceuterick, S.A., Louvain.
8. BRUGEROLLE, G. 1971. Mise en évidence du processus d'endocytose et des structures lysosomiques chez *Trichomonas vaginalis*. *C. R. Hebd. Seances Acad. Sci. Ser. D Sci. Nat. (Paris)*. **272**:2558.
9. BRUGEROLLE, G. 1972. Etudes préliminaires comparatives de 2 types de granules cytoplasmiques chez les *Trichomonas*. *J. Protozool.* **19**(Suppl.):61. (Abstr.)
10. ČERKASOVOVÁ, A. 1970. Energy-producing metabolism of *Tritrichomonas foetus*. I. Evidence for control of intensity and the contribution of aerobiosis to total energy production. *Exp. Parasitol.* **27**:165.
11. ČERKASOVOVÁ, A., and J. ČERKASOV. 1971. Localization of respiratory activity in the cell of *Tritrichomonas foetus*. *J. Protozool.* **18**(Suppl.): 44. (Abstr.)
12. CONCANNON, J. N., F. M. MILLER, and I. E. ALCAMO. 1970. Lysosomes of the trichomonads. *J. Protozool.* **17**(Suppl.):14. (Abst.)
13. CORNFORD, M. A. 1971. Ultrastructural cytochemical identification of peroxisomes as organelles of terminal oxidation in amitochondrial trichomonad flagellates. Ph.D. Thesis. Iowa State University, Ames, Iowa.
14. CORNFORD, M. A., and D. E. OUTKA. 1970. Peroxisomes as organelles of terminal oxidation in trichomonads. *J. Cell Biol.* **47**:41a. (Abstr.)
15. DANFORTH, W. F. 1967. Respiratory metabolism. *In* Research in Protozoology. T.-T. Chen, editor. Pergamon Press Ltd., Oxford. **1**:201.
16. DANIEL, W. A., C. F. T. MATTERN, and B. M. HONIGBERG. 1971. Fine structure of the mastigont system in *Tritrichomonas muris* (Grassi). *J. Protozool.* **18**:575.
17. DE DUVE, C. 1969. The peroxisome: a new cytoplasmic organelle. *Proc. R. Soc. Lond. B Biol. Sci.* **173**:71.
18. DIAMOND, L. S. 1957. The establishment of various trichomonads of animals and man in axenic cultures. *J. Parasitol.* **43**:488.
19. FILADORO, F. 1970. Ultrastructural study on the membrane of phagocytic vesicles in *Trichomonas vaginalis*. *Riv. Biol. (Perugia) (Bilingual Ed. Ital. Engl.)*. **63**:455.
20. FILADORO, F. 1970. Fine structure of chromatic granules in *Trichomonas vaginalis* Donné. *Experientia (Basel)*. **26**:213.

21. GAUMONT, R., and J. GRAIN. 1967. L'Anaerobiose et les mitochondries chez les protozoaires du tube digestif. *Ann. Univ. Assoc. Regionale Etude Tech. Sci.* **5**:174.
22. GRAIN, J. 1966. Etude cytologique de quelques Ciliés Holotriches endocommensaux des Ruminants et des Equidés. *Protistologica.* **2**(2):5.
23. HARRAP, G. J., and W. M. WATKINS. 1970. Enzymes of *Trichomonas foetus*. Separation and properties of two β-galactosidases. *Biochem. J.* **117**:667.
24. HOLLANDE, A., and J. VALENTIN. 1969. Appareil de golgi, pinocytose, lysosomes, mitochondries, bacteries symbiotiques, atractophores et pleuromitose chez les hypermastigines du genre *Joenia*. Affinites entre Joeniides et Trichomonadines. *Protistologica.* **5**:39.
25. HONIGBERG, B. M., C. F. T. MATTERN, and W. A. DANIEL. 1971. Fine structure of the mastigont system in *Tritrichomonas foetus* (Riedmuller). *J. Protozool.* **18**:183.
26. KIRBY, H. 1951. Observations on the trichomonad flagellate of the reproductive organs of cattle. *J. Parasitol.* **37**:445.
27. LASKOWSKI, M. 1955. Trypsinogen and trypsin. *Methods Enzymol.* **2**:26.
28. LEIGHTON, F., B. POOLE, H. BEAUFAY, P. BAUDHUIN, J. W. COFFEY, S. FOWLER, and C. DE DUVE. 1968. The large-scale separation of peroxisomes, mitochondria, and lysosomes from the livers of rats injected with Triton WR-1339. Improved isolation procedures, automated analysis, biochemical and morphological properties of fractions. *J. Cell Biol.* **37**:482.
29. MAEDA, N., Y. OKA, M. FURYA, Y. ITO, and H. OSAKI. 1967. Analysis of immunogenicity in protozoan cells. 24. Distribution of acid phosphatase activity in *Trichomonas foetus*. *Igaku To Seibutsugaku.* **79**:53.
30. MÜLLER, M. 1971. Lysosomes in *Tetrahymena pyriformis*. II. Intracellular distribution of several acid hydrolases. *Acta Biol. Acad. Sci. Hung.* **22**:179.
31. MÜLLER, M. 1972. Dehydrogenases in microbodies (chromatoid bodies) of *Tritrichomonas foetus*. *J. Protozool.* **19**(Suppl):30. (Abstr.)
32. OSADA, M. 1962. Electron microscopic studies on protozoa. II. Studies on *Trichomonas muris*. *Keio J. Med.* **11**:227.
33. PETERS, T. J., M. MÜLLER, and C. DE DUVE. 1972. Lysosomes of the arterial wall. I. Isolation and subcellular fractionation of cells from normal rabbit aorta. *J. Exp. Med.* **136**:1117.
34. RYLEY, J. F. 1955. Studies on the metabolism of the protozoa. 5. Metabolism of the parasitic flagellate *Trichomonas foetus*. *Biochem. J.* **59**:361.
35. SHARMA, N. N., and G. H. BOURNE. 1963. Studies on the histochemical distribution of oxidative enzymes in *Trichomonas vaginalis*. *J. Histochem. Cytochem.* **11**:628.
36. SHARMA, N. N., and G. H. BOURNE. 1964. Histochemical studies on the distribution of DPN and TPN diaphorases, β-glucuronidase and some enzymes associated with the Krebs cycle in *Trichomonas vaginalis*. *Histochemie.* **3**:487.
37. SHARMA, N. N., and G. H. BOURNE. 1964. Studies on the histochemical distribution of hydrolases in *Trichomonas vaginalis*. *Acta Histochem.* **18**:213.
38. SHORB, M. S. 1964. The physiology of trichomonads. *In* Biochemistry and Physiology of Protozoa. S. H. Hutner, editor. Academic Press, Inc., New York. **3**:383.
39. SIMPSON, C. F., and F. H. WHITE. 1964. Structure of *Trichomonas foetus* as revealed by electron microscopy. *Am. J. Vet. Res.* **25**:815.
40. SMITH, B. F., and B. T. STEWART. 1966. Fine structure of *Trichomonas vaginalis*. *Exp. Parasitol.* **19**:52.
41. TANAKA, K. 1971. Biochemical studies on dehydrogenases in *Trichomonas vaginalis*. *Kiseichugaku Zasshi.* **20**:148.
42. WATKINS, W. M. 1958. Enzymes of *Trichomonas foetus*. The action of cell-free extracts on blood-group substances and low-molecular-weight glycosidases. *Biochem. J.* **71**:261.
43. WATTIAUX, R., and C. DE DUVE. 1956. Tissue fractionation studies. 7. Release of bound hydrolases by means of Triton X-100. *Biochem. J.* **63**:606.
44. YAMAZAKI, R. K., and N. E. Tolbert. 1969. Malate dehydrogenase in leaf peroxisomes. *Biochim. Biophys. Acta.* **178**:11.